University Library

MINERVA ACCESS

A gateway to Melbourne's research publications

Minerva Access is the Institutional Repository of The University of Melbourne

Author/s:
Chen, GQ;Gras, SL;Kentish, SE

Title:
Eutectic freeze crystallization of saline dairy effluent

Date:
2020-04-15

Citation:
Chen, G. Q., Gras, S. L. & Kentish, S. E. (2020). Eutectic freeze crystallization of saline dairy effluent. Desalination, 480, https://doi.org/10.1016/j.desal.2020.114349.

Persistent Link:
https://hdl.handle.net/11343/237423

# Eutectic Freeze Crystallization of Saline Dairy Effluent

G. Q. Chen[1], S. L. Gras[1,2], S. E. Kentish[1]*

[1] The ARC Dairy Innovation Hub, Department of Chemical Engineering, University of Melbourne, Victoria 3010, Australia.

[2] The Bio21 Molecular Science and Biotechnology Institute, The University of Melbourne, Parkville, Victoria 3010, Australia

*Keywords:* Dairy; whey; Eutectic temperature; Phase diagram; Sodium chloride.

*Corresponding Author

Prof S. Kentish

Tel: +61 3 8344 6682

Fax: +61 3 8344 4153

E-mail address: sandraek@unimelb.edu.au

# ABSTRACT

The disposal of saline effluent in the dairy industry is subject to increasingly strict regulatory requirements. In this work, eutectic freeze crystallization (EFC) was investigated as a mechanism for the simultaneous separation of salts and ice in a typical saline effluent, namely salty whey. Experiments were conducted using salty whey samples collected from a dairy processing facility. The eutectic point of the salty whey was determined using differential scanning calorimetry and was found to be lower than that of NaCl solutions (–24°C for salty whey vs. –21 °C for aqueous NaCl solutions). Crystallization experiments were then used to construct the phase diagram of this dairy stream under equilibrium conditions. The change in cation composition in the supernatant at the eutectic temperature was measured as a function of time and showed that pure NaCl salts and ice formed within five minutes after this temperature was reached. The energy consumption of this process was estimated to be ~120 kWh/tonne for salty whey, which is comparable to that for conventional thermal crystallization of brine.

# 1. INTRODUCTION

Salt is a key component within dairy manufacturing, both as a result of the natural mineral levels in milk but also as sodium chloride directly added during cheese making [1]. For example, sodium chloride is added to the cheese curd to lower the water activity within the curd, when making semi-hard or hard cheeses such as Cheddar or Colby. Only about 35-50% of the added salt is retained in the curd. The excessive moisture is expelled from the curd during salting and pressing processes, together with a significant amount of the added salt, forming salty whey. Salty whey is one of several effluent streams generated by the dairy industry that is subject to increasingly strict regulatory requirements for disposal, due to the increase in agricultural water usage and local land degradation caused by sodium leaching. Thermal evaporation and membrane processes are commonly employed to reduce the volume of these effluent streams and to improve their quality before discharge [2].

Salty effluents are of low economic value and so any separation process should be performed at minimum cost. The saturation concentration of NaCl in water is 35 wt% at ambient temperature and varies little as this temperature changes [3]. This means that a large amount of water must be removed for evaporative crystallization from these effluents to occur, making this a costly approach. Freeze concentration processes have been developed as an alternative in the food and beverage manufacturing industry [4-6] as well as in the desalination industry [7, 8], to remove water in the form of ice. Such an approach can be more energetically favourable as the enthalpy of freezing is much lower than the enthalpy of evaporation (e.g., $\Delta H_{fus}$ = 334 J/g and $\Delta H_{vap}$ = 2265 J/g for water). In particular, eutectic freeze concentration (EFC) is an emerging technology that operates at the eutectic temperature of the solution to enable simultaneous separation of saline solutions into ice and salt [9], with advantages of energy reduction, high salt purity and an absence of additional chemicals [10]. EFC can overcome the limited temperature sensitivity of sodium chloride to crystallization and the high energy demand of evaporation, by reaching saturation at a lower concentration (23.3 wt%) at the eutectic temperature.

A typical phase diagram for a salt-water system is shown in Figure 1. When an unsaturated solution is cooled from point A to the temperature corresponding to its concentration on the ice line, ice begins to form in the now saturated solution. A further decrease in temperature causes the system to become more concentrated due to the crystallization of ice and to eventually reach the eutectic point, the lowest possible temperature of crystallization. At this point, crystalline salt structures and ice crystals form separately and can be separated due to the large density difference between ice (0.92 g/cm$^3$) and salts (e.g NaCl 2.17 g/cm$^3$). In a batch process, this can be observed when stirring is turned off [9]. In a continuous process, two extra separators are required, one to process the ice slurry and wash the

ice with recycled pure water, and another to wash the salt with a saturated solution [11, 12].

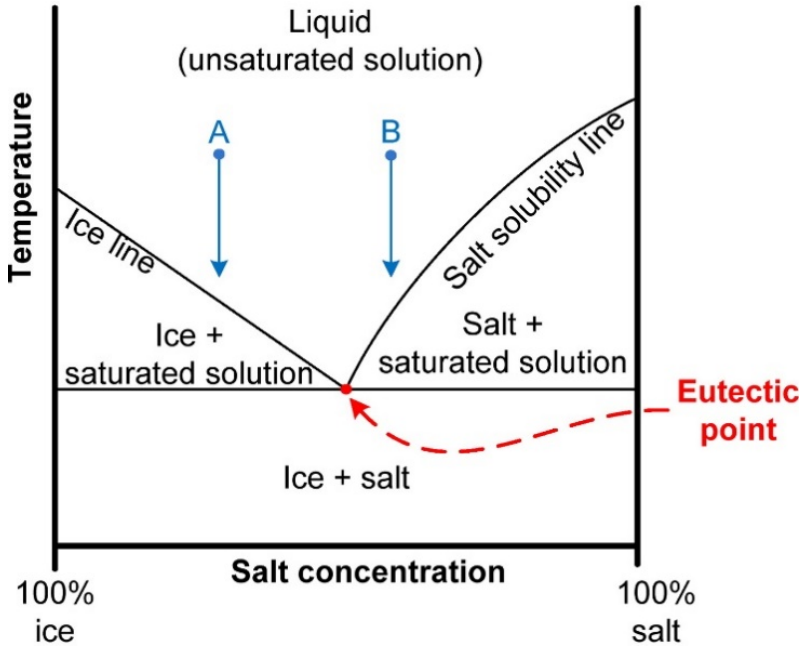



Figure 1: A typical phase diagram for aqueous salt solutions showing the Eutectic point [13]. (Copyright 2012, with permission from Elsevier.)

A life cycle assessment comparing EFC and evaporative crystallization indicated that EFC processes have great potential to reduce the energy consumption and carbon footprint of the crystallization units [14]. It was found that the EFC process consumes 6-7 times less energy when compared to evaporative crystallization for a 4 wt% model solution of sodium sulphate [14]. Van der Ham et al. [9] found that EFC could reduce the energy required to recover sodium nitrate (from 35 wt% aqueous solution) and copper sulphate (from 12 wt% aqueous solution) by 30% and 65%, respectively, compared to multi-step evaporation. Randall et al. [15] also demonstrated that EFC could convert 97% of the liquid to pure water, calcium sulphate (98.0% purity) and sodium sulphate (96.4% purity), when processing the brine stream generated by a reverse osmosis process (i.e., reverse osmosis concentrate) from the mining industry. EFC has been commercialised by a number of companies internationally. Cool Separations (The Netherlands) have developed single stage EFC that can handle multi-component systems and multi-stage EFC that can crystallise out the specific salts in sequence by operating a series of crystallisers at different temperatures. Other companies include Eskom (South Africa), PROXA Water (South Africa) and Prentec Pty Ltd (South Africa).

Salty whey from cheese manufacturing plants comprises a high concentrations of sodium chloride (50-70 wt% of the total solids [16]), with a small amount of organic matter such as milk sugar and organic

acids, as well as divalent salts such as calcium phosphate (2.5-5 wt% of total solids [16]). The composition of the fresh salty whey sample collected in this study is shown in Table 1.

In Australia, salty whey is typically managed in evaporation lagoons where water is naturally evaporated. However, the construction of further evaporation ponds in some areas is now banned due to environmental impacts from land degradation, odour and dust [2]. In this work, eutectic freeze crystallization of salts and ice from fresh salty whey samples collected from a dairy factory is carried out using a well-insulated crystallization reactor. The fresh salty whey samples are also allowed to evaporate naturally to achieve a concentration factor of 2, mimicking the brine present in the evaporation lagoons. The phase diagram, composition of supernatant and salts, as well as the energy demand for processing fresh salty whey and concentrated salty whey samples are investigated. To the best of our knowledge, this is the first study performed to demonstrate the applicability of EFC technology in processing saline effluent from the dairy industry.

# 2. EXPERIMENTAL

## 2.1 Materials

Solutions of different concentrations of sodium chloride (99.7%, AR Grade, Chem-supply Australia) were prepared in the laboratory for method validation. Salty whey samples were collected from a dairy processing facility in Victoria, Australia, after ultrafiltration (UF) was used to recover the protein. These samples are therefore referred to as salty whey (UF permeate). The composition of the salty whey (UF permeate) was typical of that commonly found in a dairy processing facility [16]. Some salty whey samples (UF permeate) obtained from a dairy company were naturally evaporated at room temperature to double the total solids content, mimicking evaporation in an evaporation pond. The pH of these concentrated samples decreased by 1 pH unit, due to the conversion of some lactose by lactic acid bacteria, as would also occur naturally in an evaporation pond. The decrease in pH caused some residual proteins to precipitate. The concentrated salty whey samples were thus filtered using a 0.22 µm Polyethersulfone (PES) filter before being processed in the crystalliser. This is referred to as evaporated and filtered (E&F) salty whey. The E&F salty whey was also diluted from 30% to 16% to study the effect of partial organic removal using the PES filter. Table 1 below shows the composition of the raw, concentrated and diluted salty whey samples.

Table 1: General characteristics and composition of salty whey (UF permeate), evaporated and filtered salty whey (E&F Salty Whey) and diluted E&F salty whey (Dil-E&F Salty Whey).

| Description | Unit | Salty Whey (UF Permeate) | Evaporated & Filtered* Salty Whey (E&F Salty Whey) | Diluted# E&F Salty Whey (Dil-E&F Salty Whey) |
|---|---|---|---|---|
| Conductivity | mS/cm | 132 ± 3 | 171 ± 3 | 137 ± 3 |
| pH | - | 5.13 ± 0.04 | 3.94 ± 0.03 | ND |
| Total Solids | % | 14.7 ± 0.1 | 30.2 ± 0.2 | 16.0 ± 0.1 |
| Ash | % | 10.8 ± 0.7 | 19.9 ± 1.3 | 10.6 ± 0.7 |
| Organic Matter | % | 3.9 ± 0.6 | 10.3 ± 1.5 | 5.4 ± 0.8 |
| Na | g/L | 41.4 ± 1.2 | 77.7 ± 2.3 | 44.3 ± 1.3 |
| K | g/L | 1.39 ± 0.05 | 3.21 ± 0.13 | 1.64 ± 0.06 |
| Mg | g/L | 0.14 ± 0.01 | 0.29 ± 0.01 | 0.14 ± 0.01 |
| Ca | g/L | 1.52 ± 0.05 | 2.43 ± 0.08 | 1.17 ± 0.04 |
| P^ | g/L | 0.74 ± 0.03 | 1.23 ± 0.05 | 0.99 ± 0.04 |

* Prepared by evaporation of salty whey (UF Permeate) at 30 ± 5 °C followed by filtration with by 0.22-micron PES (Polyethersulfone) filters

# Dilution factor: 2

^ Phosphorus (P) is present as phosphate ions. *Chloride ions (not determined) are the primary anions in the sample with a similar molar concentration to that of sodium [16].*

ND: Not determined

## 2.2 EFC Reactor

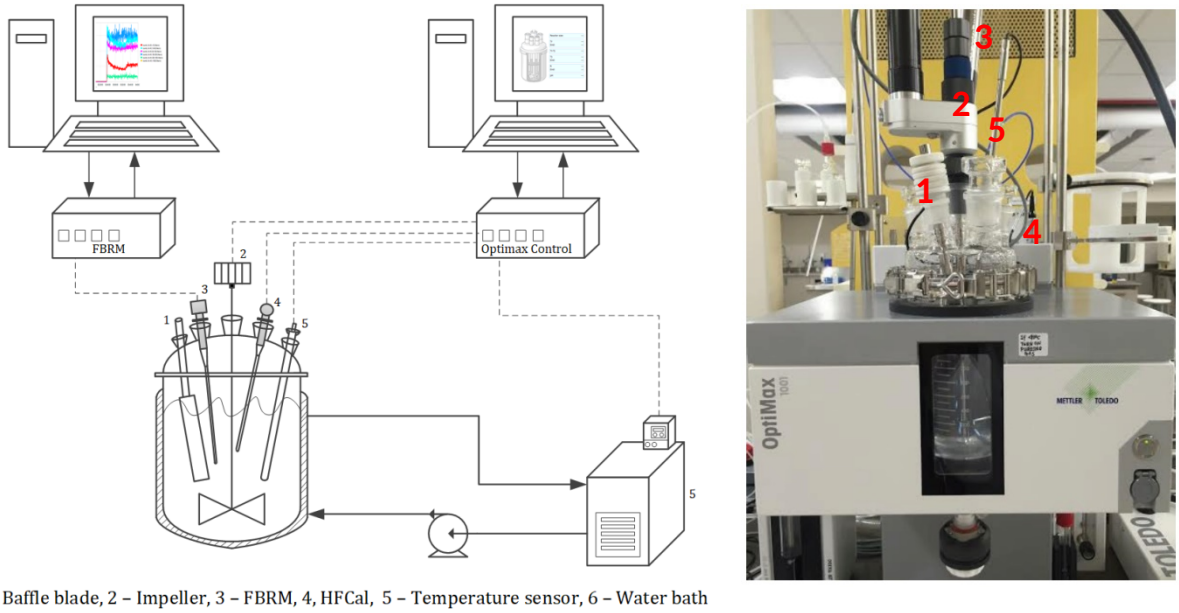
A crystallization reactor of 1 L (Optimax 1001 Mettler Toledo) was used to study the freezing process (Figure 2). The reactor can be operated from −30 °C to 180 °C, using a reactor jacket with an ethylene glycol and water mixture as the circulated cooling medium. The temperature was recorded using a temperature probe, while a calorimetric probe (OptiMax™ HFCal) was used to measure the heat flow between the reactor and the jacket. A focused beam reflectance measurement (FBRM) sensor was used to collect estimates of the particle size within a range ranging from <10 µm to ~1000 µm. It should be noted that rather than a particle diameter, the FBRM measures a chord length, which is defined as the distance between the two edges of a particle through which the beam passes [17]. Heat flow calorimetric information was used to estimate the specific heat capacity of the sample, which was performed by the built in program within the iControl™ Software.

Reactor volumes of 600 – 900 mL were used for each experiment. The reactor temperature was lowered to the desired temperature at a rate of <0.15 K/min. An overhead stirrer was used to agitate the samples within the reactor. For temperatures greater than −18 °C, a stirring speed of 300 rpm was used, while 800 – 1000 rpm was used for lower temperatures to ensure adequate mixing of the

127 solution-crystal mixture.

128 Two different approaches were used to construct the phase diagram of both the NaCl-$H_2O$ system and
129 the salty whey system. In the first approach, the temperature of solutions of different concentration
130 was lowered until crystallization occurred, while the reactor and jacket temperatures and the
131 corresponding particle size counts were monitored. The crystallization temperature was determined
132 from a rapid change in the jacket temperature as the latent heat is dissipated from the system when
133 crystallization occurs. This was confirmed by a sharp increase in the chord length counts detected by
134 the FBRM at this temperature (see Section 3.2). The crystallization temperature was then plotted
135 against the initial total solids concentrations to form the phase diagram.

136 In the second approach, solutions of a specific concentration were cooled in a stepwise manner, with
137 samples of the supernatant taken within 5 minutes of a specific reactor temperature being reached.
138 At each temperature, the stirrer was paused for 30 seconds to allow ice crystals to float to the top
139 and/or salt crystals to settle in the reactor, so that a clear supernatant could be obtained from the
140 middle section of the reactor. Once the reactor had reached the estimated eutectic temperature ( –
141 21 °C for NaCl solutions and −24 °C for salty whey) it was held at this temperature for 60 minutes
142 before a final supernatant sample was collected. The total dissolved solids concentration in the
143 supernatant was determined and was used to construct the phase diagram.




1 – Baffle blade, 2 – Impeller, 3 – FBRM, 4, HFCal, 5 – Temperature sensor, 6 – Water bath

144

145 Figure 2: The schematic of OptiMax 1001 crystalliser equipped with temperature, heat flow and FBRM
146 sensors (left); and a photo of the crystalliser without showing the water bath and computers (b).

147
148

## 2.3 Analysis

Differential Scanning Calorimetry (DSC 8500, PerkinElmer) was used to determine the eutectic temperature. The samples were sealed in aluminum pans, while an empty pan was used as reference. The samples were held at 25 °C for 5 minutes to stabilise the initial heat flow. A temperature scan from 25 °C to −80 °C was then conducted using a linear scanning rate of 3 K/min, after which the samples were heated to 25 °C at the same scanning rate.

Total dissolved solids and total ash were determined as per Australian Standards AS 2003.1.1 and AS 2003.1.5. The aqueous phase samples were weighed before drying at 110 °C overnight in an oven to evaporate all moisture. The total dissolved solids was determined from this mass balance. After weighing, the dried samples were further charred in a furnace at 650°C for more than 12 hours until samples turned white. Organic matter was calculated as the difference between the total dissolved solids and total ash content. In pure sodium chloride solutions, the total dissolved solids concentration refers to the concentration of sodium chloride. In salty whey solutions, the total dissolved solids include the organic matter and the total salts (ash) in the system, inclusive of sodium chloride and other salts such as calcium phosphate. Further, Inductively Coupled Plasma Atomic Emission Spectroscopy (ICP-OES 720ES, Varian) was used to determine the concentrations of sodium, potassium, calcium, magnesium and phosphorus within the ash.

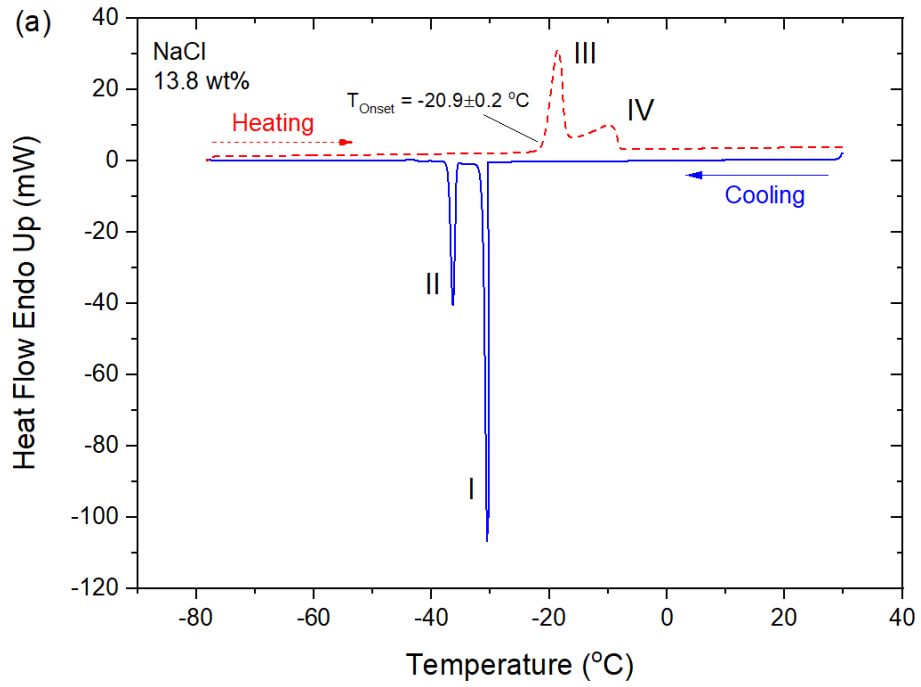
# 3. RESULTS AND DISCUSSION

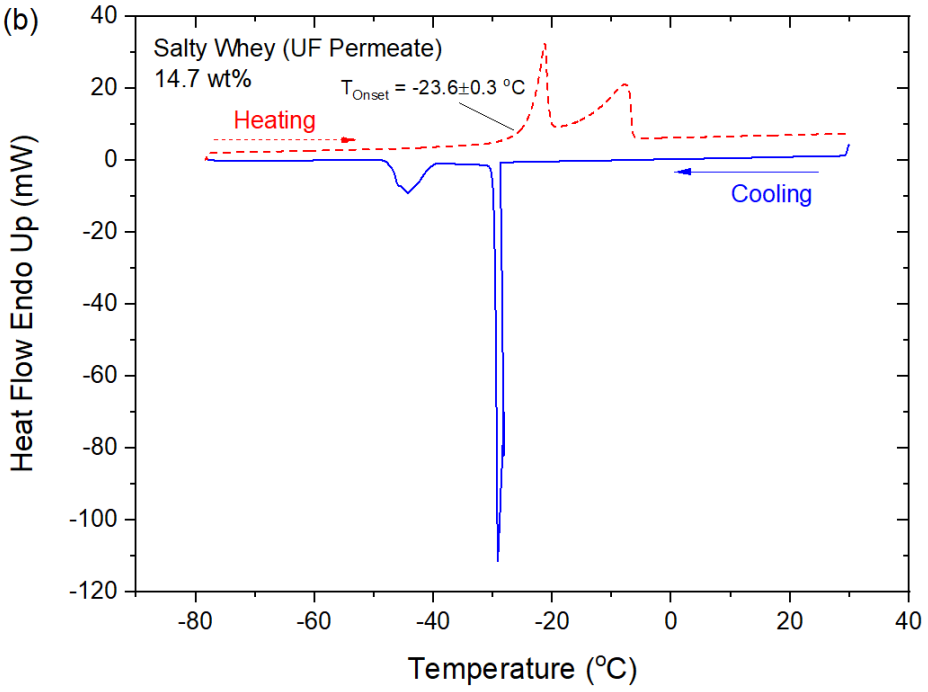
## 3.1 Eutectic Temperature

DSC thermograms were used to determine the eutectic temperature. The technique was initially used with pure sodium chloride to validate the method and determine its precision. Figure 3 (a) shows the DSC thermograms of a 13.8% NaCl solution, which is indeed consistent with the literature [18, 19]. The first transition temperature T(I) on the cooling curve is the temperature at which ice crystals appear in the solution. T(II) represents the non-equilibrium crystallization of NaCl from a super-saturated solution, which is much lower than the equilibrium eutectic temperature (i.e. −36°C versus −21 °C). This is typical behavior observed during cooling of NaCl solutions[18]. During heating, the transition temperature T(III) represents the true eutectic temperature of NaCl (−20.9 ± 0.2°C) as these crystals melt, while transition IV is caused by the melting of ice in the sample at ~0°C.

Given salty whey contains mostly sodium chloride, the eutectic freeze temperature of salty whey is expected to be similar to a NaCl-$H_2O$ system. Samples of salty whey (UF permeate) and evaporated &

filtered salty whey were also scanned by the DSC to produce similar thermograms (Figures 3(b) and (c)). It can be seen that both samples show similar heat flow curves during heating and cooling, with the eutectic point of the salty whey samples collected for this study being −23.6 ± 0.3 °C for salty whey (UF permeate) and −24.2 ± 0.3 °C for evaporated & filtered salty whey.



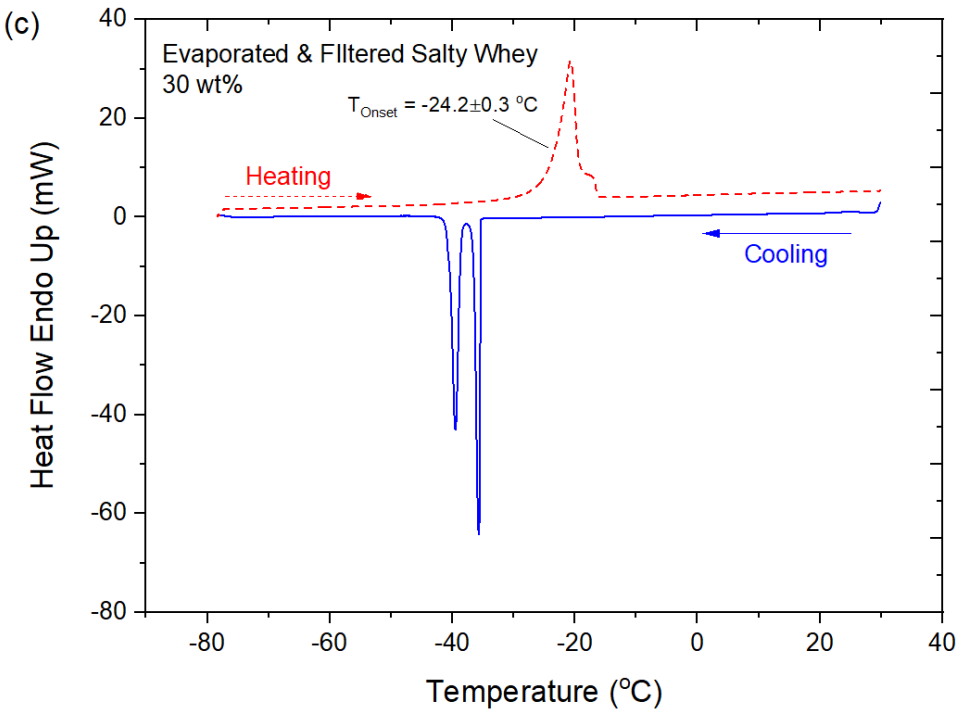



Figure 3: DSC thermograms (heat flow vs. temperature) measured during cooling (I and II) from 30°C to −80 °C and subsequent heating (III and IV) for (a) 13.8% NaCl in water, (b) salty whey (UF permeate) and (c) evaporated & filtered salty whey. The scanning rate was 3°C/min for both cooling and heating steps. The eutectic temperatures were determined to be −20.9 ± 0.2 °C, −23.6 ± 0.3 °C, and −24.2 ± 0.3 °C for 13.8% NaCl in water, salty whey (UF permeate) and evaporated & filtered salty whey, respectively.

## 3.2 Phase diagram

The phase diagram for the NaCl-$H_2O$ system was first validated against the data generated by the Extended UNIQUAC model to verify the effectiveness and the reproducibility of the experiments.

The equilibrium solubility for NaCl-$H_2O$ was first obtained by the first approach described in Section 2.2, that of cooling NaCl solutions with known concentration from room temperature to −21 °C in the crystallization reactor. The formation of salt or ice crystals in the reactor could be identified from the change of either the cooling profile or the FBRM particle count. As an example, the temperature profile of the crystallization reactor and the jacket for 18.7 wt% NaCl is presented in Figure 4 (a). It can be seen that as crystallization occurs, a significant change in the temperature difference between the reactor and the jacket ($T_r$-$T_j$) is detected at 6800 s. This change can be attributed to the formation of ice crystals, as the additional latent heat released means that the jacket temperature must be lowered at a more rapid rate to maintain the cooling rate setpoint (0.15 K/min). This also corresponds to a sharp increase in the particle size counts at 6800 s due to the presence of ice crystals, as shown in Figure 4 (b). The reactor temperature at which the significant changes in ($T_r$-$T_j$) and the particle size

occur is the crystallization temperature (i.e., −15 °C for 18.7 wt% NaCl). These experiments were repeated for a range of NaCl concentrations and the corresponding crystallization temperatures were plotted against these concentrations to form the equilibrium solubility line in the phase diagram (black circles in Figure 5).

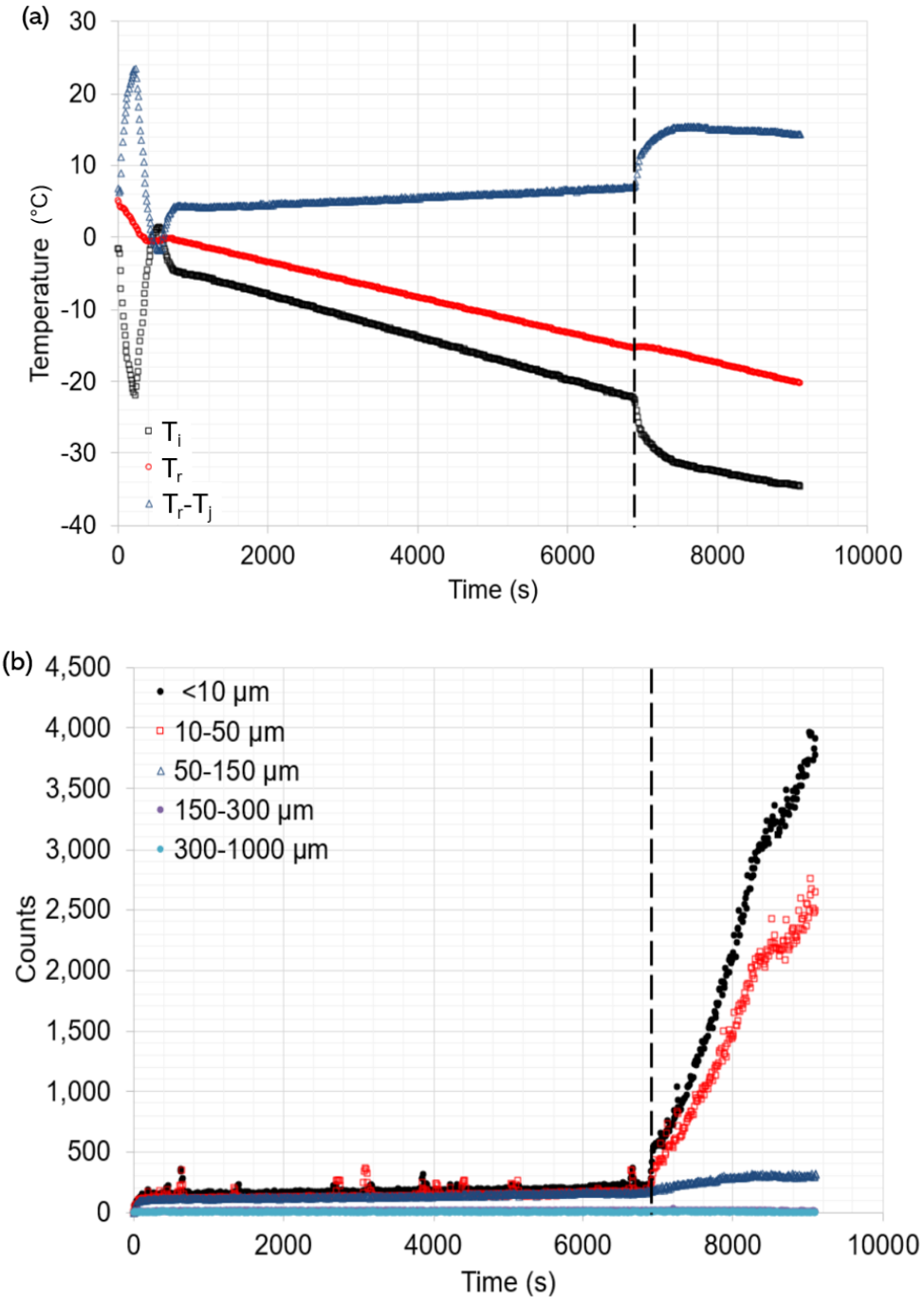



Figure 4: Temperature profile of the reactor (a) and counts of particles of various size (in µm) within the reactor (b) during the crystallization of NaCl (18.7 wt%) using the OptiMax 1001 crystalliser. ($T_j$: Jacket Temperature; $T_r$: Reactor Temperature). Crystallization occurs at 6800 s on the timeline.

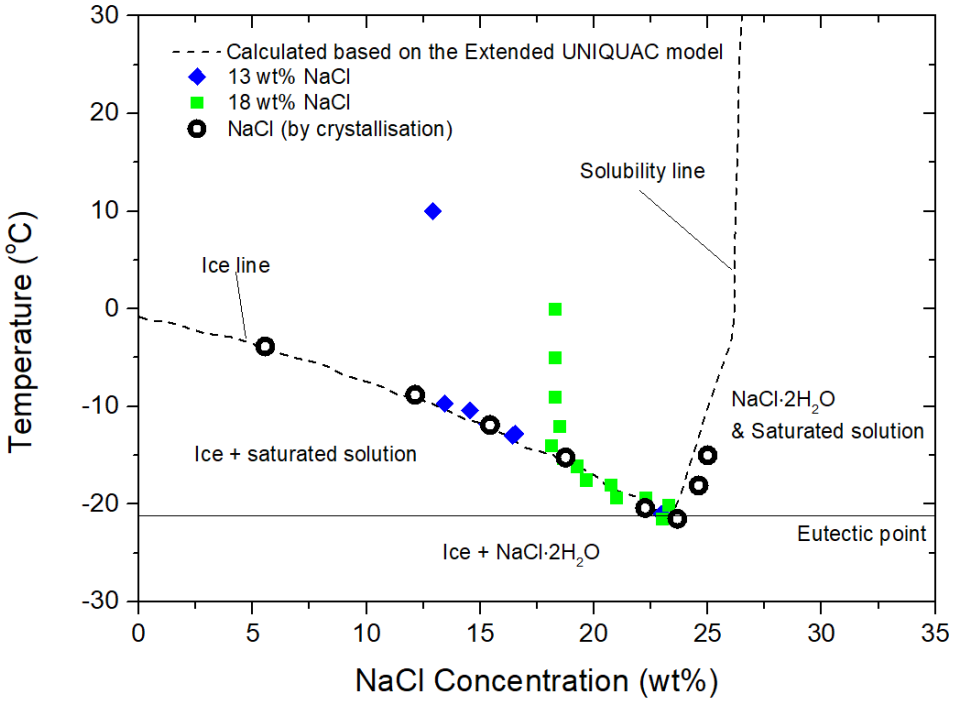



Figure 5: Phase diagram of the NaCl-$H_2O$ system. The crystallization temperatures of NaCl solutions of different concentrations, determined using the first approach detailed in Section 2.2 are plotted as black circles. The concentration of NaCl at different reactor temperatures, cooling from room temperature at initial concentrations of 13 wt% (blue diamonds) and 18 wt% (green squares) was estimated using the second approach detailed in Section 2.2. The phase diagram generated based on the Extended UNIQUAC model is shown as the dashed line.

A second approach to develop the phase diagram was to measure the total solids concentration in the supernatant. As shown in Figure 5, NaCl solutions of 13 wt% and 18 wt% were cooled from room temperature to −20 °C. Samples of the supernatant were collected from the middle of the reactor at different reactor temperatures, after the stirrer was paused to allow ice to float to the top of the mixture. The total dissolved solids concentration in these supernatant samples was determined and was plotted against the corresponding reactor temperature in the phase diagram. Data generated from both approaches are in agreement with the phase diagram for the NaCl-$H_2O$ system calculated using the Extended UNIQUAC model (Figure 5), illustrating the effectiveness of either approach in developing the phase diagram using the Optimax 1001 crystalliser.

Salty whey from the dairy processing plant is not available as fresh samples in different concentrations. As it is a waste effluent, it is also not available in powder form for re-constitution into solutions of different concentration. Therefore, the second approach was employed as the primary mechanism to generate the phase diagram for salty whey. In order to determine the total dissolved solids concentration of the supernatant, supernatant samples of salty whey (UF permeate) at different

temperatures were collected within 5 minutes after a certain reactor temperature was reached. To understand if the system was in equilibrium when these samples were collected, the reactor temperature was also held at specific temperatures for 1 hour. As shown in Figure 6, within the experimental error of the total dissolved solids concentration measurements and the variation of the reactor temperature, it can be regarded that system equilibrium is achieved within the first five minutes.

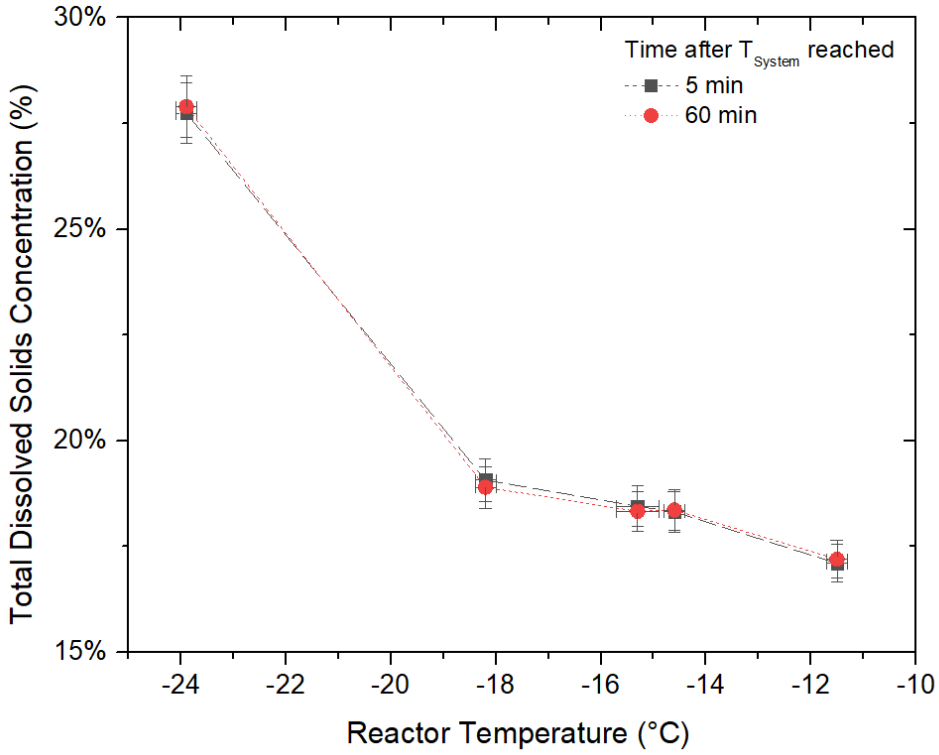



Figure 6: Total dissolved solids concentrations in salty whey (UF permeate) 5 min and 60 min after the reactor temperature was reached. Lines are drawn to guide the eye.

The phase diagram for salty whey was successfully constructed using this approach (Figure 7). Fresh salty whey (UF permeate) samples (~15 wt%) and the concentrated and filtered salty whey sample (~30 wt%) were cooled from room temperature to −24 °C. Total solids concentration in the supernatant for salty whey (UF permeate) increased from 14.8% ± 0.1% to 29.1% ± 0.2%, as ice crystals formed in the reactor during the cooling process. Conversely, during the cooling process of the E&F salty whey sample, salt crystallization occurred, leading to a decrease in total solids concentration in the supernatant. The cooling curve from the fresh salty whey (UF permeate) samples forms the ice line (as defined in Figure 1), while the curve obtained from the E&F salty whey samples is the solubility line (as defined in Figure 1) of salty whey.

It is noted that the data points for salty whey samples scatter slightly near the eutectic temperature in Figure 7, although within the measurement sensitivity of both parameters. This is probably because complete crystallization of the small quantities of calcium phosphate present in the solution can take up to 168 hours (i.e. 1 week) [20]. To validate the phase diagram, the freezing curve for the diluted E&F salty whey samples was also determined. The resulting ice line is consistent with that of the original salty whey permeate (Figure 7). This also means that natural evaporation of salty whey in solar ponds, which only concentrates the brine, would have little influence on the thermal properties in the process of eutectic freeze concentration.

It should be noted that the current refrigeration systems (ammonia based) in the dairy industry have the capacity to provide a cooling temperature of no lower than −20°C [7]. Hence, if spare cooling load is available within the dairy processing facilities, one of the immediate opportunities for ice/water recovery from salty whey could be considered at a temperature higher than the eutectic temperature (e.g., −15°C), where up to 40% of water (from 13%TS at >0°C to 21%TS at −15°C, see Figure 7) can be recovered as pure frozen water during a freeze concentration process.

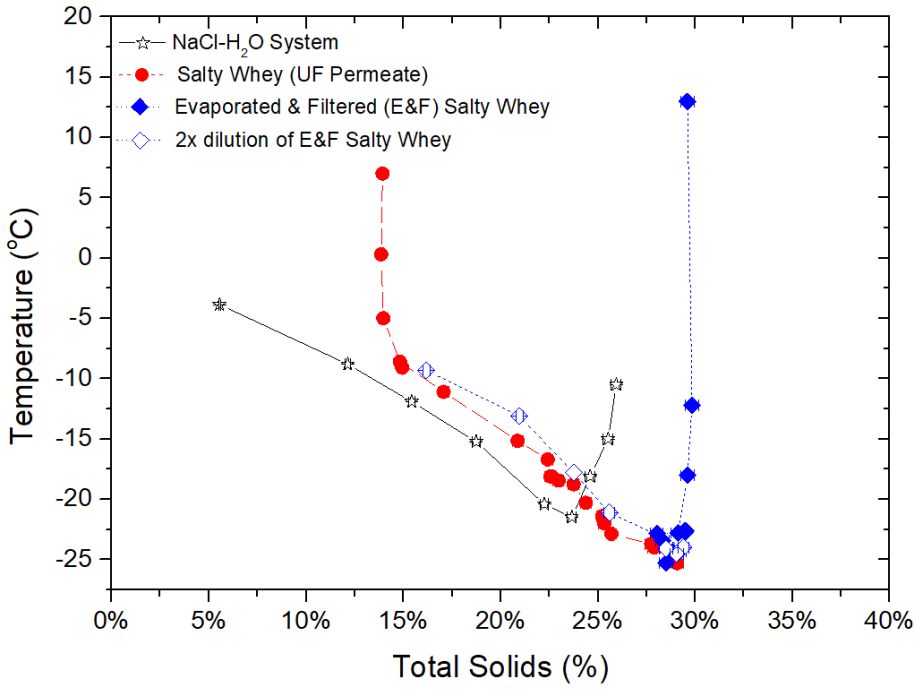



Figure 7: Phase diagram of aqueous sodium chloride solution, salty whey (UF permeate), E&F salty whey and diluted E&F salty whey. Lines are drawn to guide the eye.

At the eutectic temperature, a complete separation of ice and salt crystals was not visually observed with the current reactor setup. This is because an 'ice jacket' (i.e., scaling) formed around the inner wall of the reactor. This scaling layer covered the limited observation window of the Optimax 1001

reactor and hence did not allow observation of such phenomena. Preliminary information on the size of crystals during the freezing process, was however obtained by Focused Beam Reflectance Measurement (FBRM). At different solution stirring speeds, the particle size distribution varies (Figure 8). The low stirring speed (Figure 7 A and C, 300 rpm) was only used for reactor temperatures above −18 °C. At −18°C, the NaCl-$H_2O$ system has a broad distribution of crystals (Figure 7 A, median chord length: 25 microns), while the salty whey system produced a bimodal distribution with crystals of chord length 7 microns and 20 microns (Figure 7C). To allow the reactor temperature to go below −18°C, the stirring speed was then raised to overcome the increased heat transfer resistance caused by both the thick 'ice jacket' formed around the inner reactor wall and the increased viscosity of the solution/crystal mixture. At high stirring speeds, air bubbles were inevitably introduced in the system hence a clear particle size distribution could not be obtained. It can be seen, however, that the salty whey system produces smaller crystals (5-20 microns) than the NaCl-$H_2O$ system (~100 microns). The 100-micron particles in the NaCl-$H_2O$ system were produced probably because the system temperature was allowed to go beyond its eutectic point (−24°C vs −21°C).

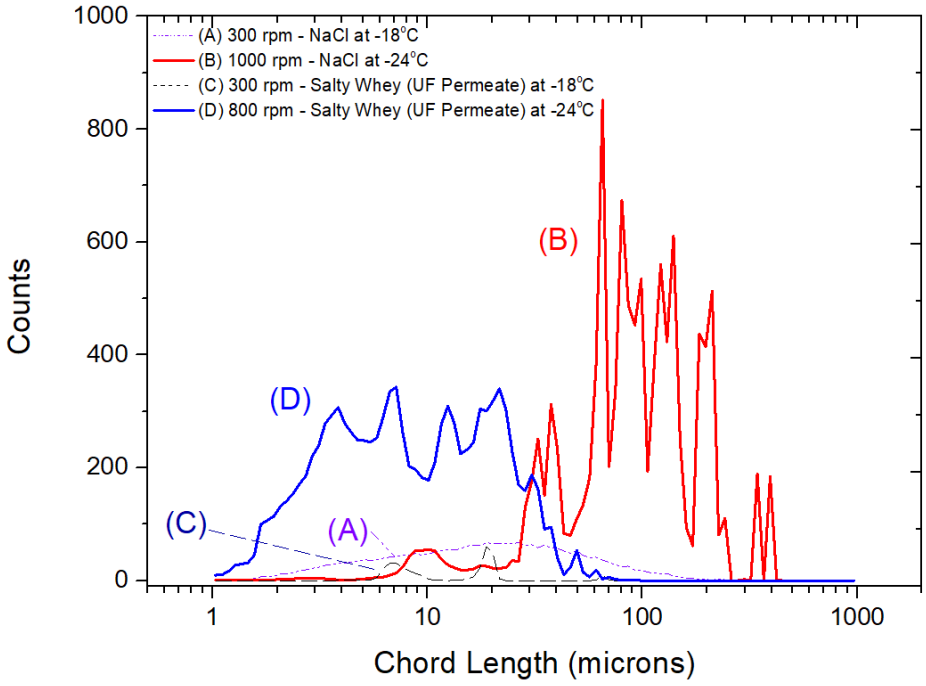



Figure 8: Chord length distribution of crystals for NaCl solutions and salty whey at −18°C and −24°C at different stirrer speeds.

The composition of salt crystals created one hour after the eutectic temperature is reached was also determined indirectly from the changes in the supernatant composition. As seen in Figure 9 , for both the salty whey (UF permeate) and the E&F salty whey samples, the ratio of Na/K decreases, whereas the ratios of Ca/K and P/K remain constant at the eutectic temperature. This indicates that the crystals

formed at the eutectic temperature are sodium salts. This is consistent with the very slow kinetics for calcium phosphate precipitation at low temperatures, as shown in our previous study [10]. Industrial scale EFC processes separate the crystals and supernatant continuously as ice and salt crystals are formed [13, 21]. This implies that potentially pure sodium chloride salt and clean water can be simultaneously recovered from salty whey using a eutectic freeze concentration process, leaving a residual effluent that is more concentrated in calcium phosphate.

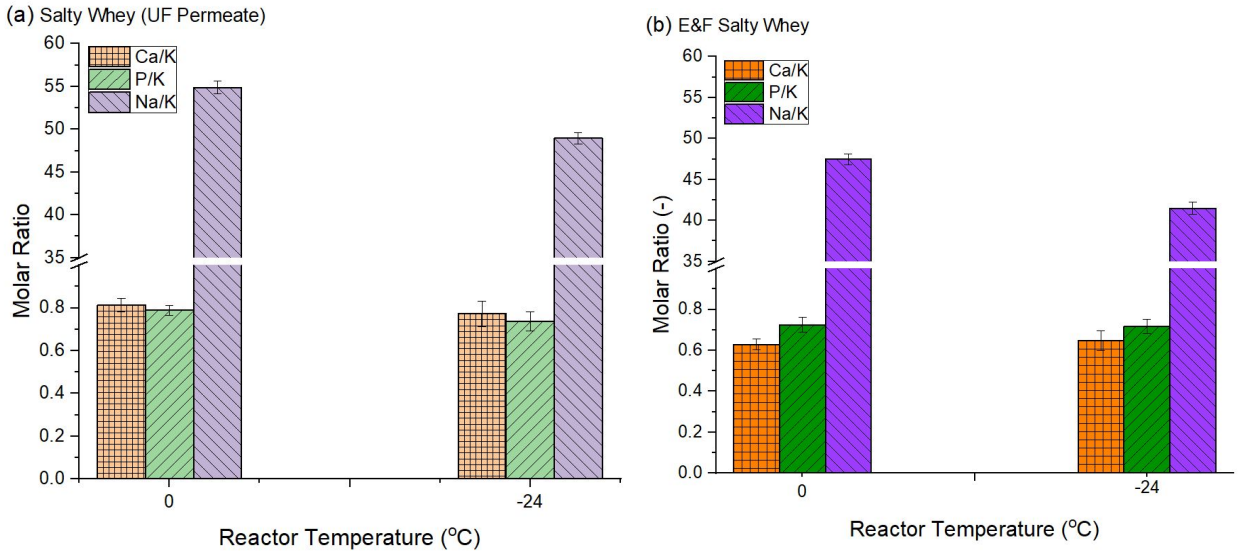



Figure 9: Molar ratio of calcium, phosphorus and sodium to potassium in the supernatant for (a) salty whey (UF permeate) and (b) evaporated and filtered salty whey samples at 0 and −24 °C.

## 3.3 Energy consumption

The energy consumption of a continuous EFC process processing 5 wt%, 15 wt% and 30 wt% NaCl, as well as 15 wt% and 30 wt% salty whey, was estimated using the energy analysis approach reported by Van der Ham [9]. It is assumed that the process separates continuously sodium chloride salts from water, with 100% recovery and no heat loss in the system. The theoretical minimum energy requirement for an ideal EFC process was calculated as the sum of the energy requirement for cooling the feed to the eutectic temperature and the cooling required to achieve the phase changes to solid ice and salt.

The sensible heat required to cool the solution from 20 °C to its eutectic temperature was determined based on the specific heat capacity of sodium chloride and salty whey presented in Figure 10. The specific heat capacity of 26.3 wt% sodium chloride and salty whey (15% and 30%) was estimated using the calorimetric probe (OptiMax™ HFCal). Both literature data and the measured values show very

small variations in the heat capacity with respect to temperature. The cooling requirement for ice and salt formation was estimated based on the enthalpy of crystallization/formation of ice (6.012 kJ/mol) and sodium chloride dihydrate (6.8 kJ/mol, averaged from values reported in Drebushchak and Ogienko [22], Verbeek [23] and Swenne [24]).

As shown in Figure 11, the minimum energy required is similar between pure NaCl solutions and salty whey with the same total solids concentrations, since salty whey contains primarily NaCl. Increasing the salty whey concentration from 15wt% to 30wt% reduces the energy demand by 11% (from 125 kWh/tonne feed to 111 kWh/tonne feed). This is due to the reduced latent heat required to generate ice crystals as there is less water present, as well as the lower specific heat capacity of solutions at higher concentrations (Figure 10). The estimate from the ideal case presented in Verrbeek [23] for 5 wt% solution is slightly higher, because Verrbeek took into consideration the washing of ice and salt downstream in a wash column and a belt filter. For optimized thermal brine concentrator-crystalliser systems, >80 kWh/m$^3$ feed (<65,000 ppm, equiv. to ~6 wt%) is required [25] which is a little less than that presented in Figure 11. It should be noted that EFC is still an emerging technology and improvement in process design and energy integration could result in enhanced energy efficiency in the future.

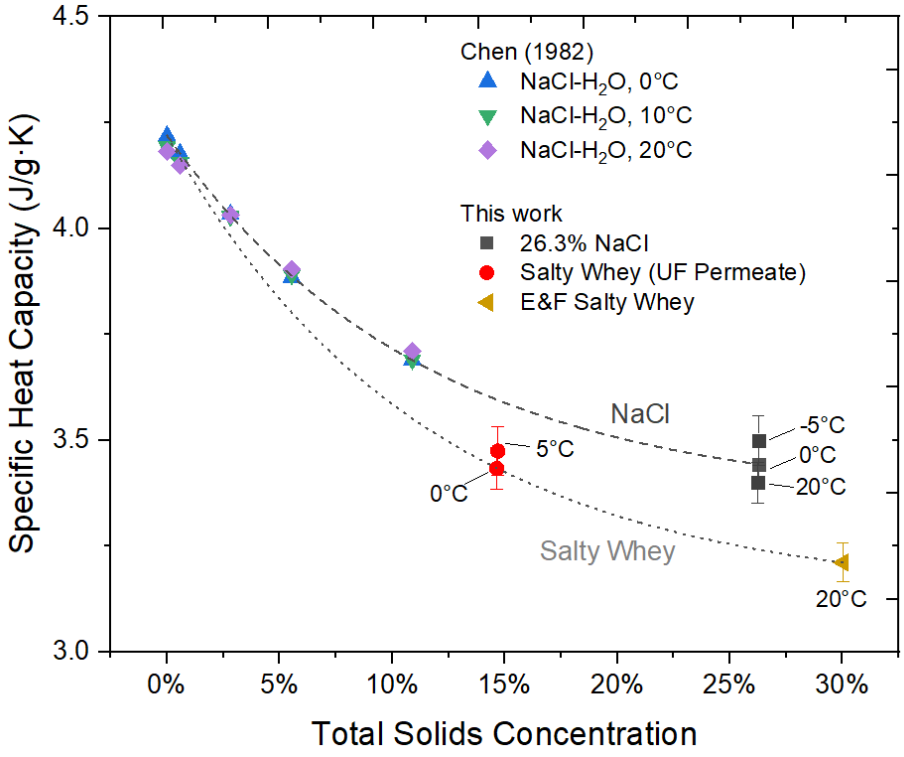



Figure 10: Specific heat capacity of NaCl solutions of different concentrations reported in the literature by Chen [26] and that of 26.3 wt% NaCl and salty whey samples measured in this work using the calorimetric probe (OptiMax™ HFCal). Lines are drawn to guide the eye.

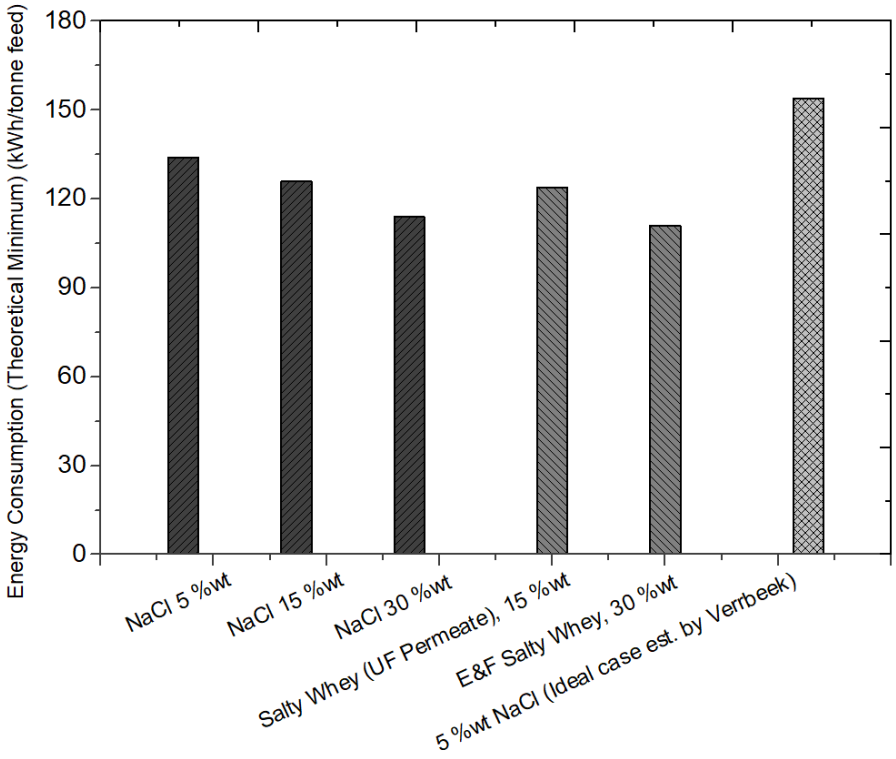



Figure 11: Theoretical minimum energy required for processing one tonne of different brine solutions by EFC with 100% water and NaCl recovery. Data for the 5 wt% NaCl ideal case is reported by Verbeek [23].

## 4. CONCLUSIONS

Fresh salty whey samples collected from a dairy processing facility in Victoria, Australia were used to construct the solid-liquid phase diagram of salty whey under equilibrium conditions. The eutectic point of salty whey was found to be at −24°C, lower than that of NaCl solutions (−21 °C). The temperature-total solids concentration relationship is similar, however, to that attained for these aqueous sodium chloride solutions. Pure NaCl salts and ice were formed within 5 minutes after the eutectic temperature was reached, as determined by monitoring the changes of cation composition in the supernatant at the eutectic temperature. The lower eutectic temperature makes it difficult for eutectic freeze crystallization to be operated with ammonia-based refrigeration systems and hence simple freeze crystallization at −15°C may be more attractive. The energy consumption of the eutectic freeze crystallization process was estimated to be in the range of 111 to 125 kWh/tonne for salty whey samples (15 wt% and 30 wt%). This energy demand could potentially be reduced through energy integration with onsite refrigeration processes. The energy requirement for cooling the dairy brine solutions to their eutectic point is in the same order of magnitude as that for using conventional

thermal brine concentrators and crystallisers (80 kWh per tonne feed).

## ACKNOWLEDGEMENT

The Australian Research Council's Industrial Transformation Research Program (ITRP) funding scheme (project number IH120100005). The ARC Dairy Innovation Hub is a collaboration between The University of Melbourne, The University of Queensland and Dairy Innovation Australia Ltd.

## REFERENCES

[1] G.Q. Chen, S.L. Gras, S.E. Kentish, Separation Technologies for Salty Wastewater Reduction in the Dairy Industry, Separation & Purification Reviews, (2018) 1-29.
[2] G.Q. Chen, S. Talebi, S.L. Gras, M. Weeks, S.E. Kentish, A review of salty waste stream management in the Australian dairy industry, J. Environ. Manage., 224 (2018) 406-413.
[3] P. Bharmoria, H. Gupta, V.P. Mohandas, P.K. Ghosh, A. Kumar, Temperature Invariance of NaCl Solubility in Water: Inferences from Salt–Water Cluster Behavior of NaCl, KCl, and NH4Cl, The Journal of Physical Chemistry B, 116 (2012) 11712-11719.
[4] D.R. Heldman, D.B. Lund, C. Sabliov, Handbook of Food Engineering, CRC Press, 2006.
[5] R.W. Hartel, L.A. Espinel, Freeze concentration of skim milk, J. Food Eng., 20 (1993) 101-120.
[6] M.V. Rane, D.B. Uphade, Energy Efficient Jaggery Making Using Freeze Pre-concentration of Sugarcane Juice, Energy Procedia, 90 (2016) 370-381.
[7] P. Williams, M. Ahmad, B. Connolly, Freeze desalination: An assessment of an ice maker machine for desalting brines, Desalination, 308 (2013) 219-224.
[8] P.M. Williams, M. Ahmad, B.S. Connolly, D.L. Oatley-Radcliffe, Technology for freeze concentration in the desalination industry, Desalination, 356 (2015) 314-327.
[9] F. van der Ham, G.J. Witkamp, J. de Graauw, G.M. van Rosmalen, Eutectic freeze crystallization: Application to process streams and waste water purification, Chemical Engineering and Processing: Process Intensification, 37 (1998) 207-213.
[10] S.T. Reddy, A.E. Lewis, G.J. Witkamp, H.J.M. Kramer, J. van Spronsen, Recovery of Na2SO4·10H2O from a reverse osmosis retentate by eutectic freeze crystallization technology, Chem. Eng. Res. Des., 88 (2010) 1153-1157.
[11] R.J.C. Vaessen, B.J.H. Janse, M.M. Seckler, G.J. Witkamp, Evaluation of the Performance of a Newly Developed Eutectic Freeze Crystallizer: Scraped Cooled Wall Crystallizer, Chem. Eng. Res. Des., 81 (2003) 1363-1372.
[12] J. Van Spronsen, M.R. Pascual, F.E. Genceli, D.O. Trambitas, H. Evers, G.J. Witkamp, Eutectic freeze crystallization from the ternary Na2CO3–NaHCO3–H2O system: A novel scraped wall crystallizer for the recovery of soda from an industrial aqueous stream, Chem. Eng. Res. Des., 88 (2010) 1259-1263.
[13] M.J. Fernández-Torres, F. Ruiz-Beviá, M. Rodríguez-Pascual, H. von Blottnitz, Teaching a new technology, eutectic freeze crystallization, by means of a solved problem, Education for Chemical Engineers, 7 (2012) e163-e168.
[14] M.J. Fernández-Torres, D.G. Randall, R. Melamu, H. von Blottnitz, A comparative life cycle assessment of eutectic freeze crystallization and evaporative crystallization for the treatment of saline wastewater, Desalination, 306 (2012) 17-23.
[15] D.G. Randall, J. Nathoo, A.E. Lewis, A case study for treating a reverse osmosis brine using Eutectic Freeze Crystallization—Approaching a zero waste process, Desalination, 266 (2011) 256-262.

[16] K. Kezia, J. Lee, M. Weeks, S. Kentish, Direct contact membrane distillation for the concentration of saline dairy effluent, Water Res., 81 (2015) 167-177.
[17] A. Ruf, J. Worlitschek, M. Mazzotti, Modeling and Experimental Analysis of PSD Measurements through FBRM, Particle & Particle Systems Characterization, 17 (2000) 167-179.
[18] A. Hvidt, K. Borch, NaCl-H2O Systems at temperatures below 273 k, studied by differential scanning calorimetry, Thermochim. Acta, 175 (1991) 53-58.
[19] P.H. Rasmussen, B. Jørgensen, J. Nielsen, Aqueous solutions of proline and NaCl studied by differential scanning calorimetry at subzero temperatures, Thermochim. Acta, 303 (1997) 23-30.
[20] K. Kezia, J. Lee, B. Zisu, G.Q. Chen, S.L. Gras, S.E. Kentish, Solubility of Calcium Phosphate in Concentrated Dairy Effluent Brines, Journal of Agricultural and Food Chemistry, 65 (2017) 4027-4034.
[21] F.E. Genceli, Scaling-Up Eutectic Freeze Crystallization, in: Mechanical Maritime and Materials Engineering, Technische Universiteit Delft, 2008.
[22] V.A. Drebushchak, A.G. Ogienko, Calorimetric measurements of sodium chloride dihydrate (hydrohalite), J. Therm. Anal. Calorim., (2019).
[23] B. Verbeek, Eutectic Freeze Crystallization on Sodium Chloride, Analysis of a full experimental cycle, in: Faculty of Process Equipment, Delft University of Technology, Netherlands, 2011.
[24] D.A. Swenne, The eutectic crystallization of NaCl.2H2O and ice, in: Department of Chemical Engineering and Chemistry, Technische Hogeschool Eindhoven, 1983.
[25] M. Mickley, Survey of high-recovery and zero liquid discharge technologies for water utilities, in, Water Reuse Foundation, 2008.
[26] C.T.A. Chen, Specific heat capacities of aqueous sodium chloride solutions at high pressures, Journal of Chemical & Engineering Data, 27 (1982) 356-358.

# Tables

Table 1: General characteristics and composition of salty whey (UF permeate), evaporated and filtered salty whey (E&F Salty Whey) and diluted E&F salty whey (Dil-E&F Salty Whey).

## Figure Captions

Figure 1: A typical phase diagram for aqueous salt solutions showing the Eutectic point [13]. (Copyright 2012, with permission from Elsevier.)

Figure 2: The schematic of OptiMax 1001 crystalliser equipped with temperature, heat flow and FBRM sensors (left); and a photo of the crystalliser without showing the water bath and computers (b).

Figure 3: DSC thermograms (heat flow vs. temperature) measured during cooling (I and II) from 30°C to −80 °C and subsequent heating (III and IV) for (a) 13.8% NaCl in water, (b) salty whey (UF permeate) and (c) evaporated & filtered salty whey. The scanning rate was 3°C/min for both cooling and heating steps. The eutectic temperatures were determined to be −20.9 ± 0.2 °C, −23.6 ± 0.3 °C, and −24.2 ± 0.3 °C for 13.8% NaCl in water, salty whey (UF permeate) and evaporated & filtered salty whey, respectively.

Figure 4: Temperature profile of the reactor (a) and counts of particles of various size (in µm) within the reactor (b) during the crystallization of NaCl (18.7 wt%) using the OptiMax 1001 crystalliser. ($T_j$: Jacket Temperature; $T_r$: Reactor Temperature). Crystallization occurs at 6800 s on the timeline.

Figure 5: Phase diagram of the NaCl-$H_2O$ system. The crystallization temperatures of NaCl solutions of different concentrations, determined using the first approach detailed in Section 2.2 are plotted as black circles. The concentration of NaCl at different reactor temperatures, cooling from room temperature at initial concentrations of 13 wt% (blue diamonds) and 18 wt% (green squares) was estimated using the second approach detailed in Section 2.2. The phase diagram generated based on the Extended UNIQUAC model is shown as the dash line.

Figure 6: Total dissolved solids concentrations in salty whey (UF permeate) 5 min and 60 min after the reactor temperature was reached. Lines are drawn to guide the eye.

Figure 7: Phase diagram of aqueous sodium chloride solution, salty whey (UF permeate), E&F salty whey and diluted E&F salty whey. Lines are drawn to guide the eye.

Figure 8: Chord length distribution of crystals for NaCl solutions and salty whey at −18°C and −24°C at different stirrer speeds.

Figure 9: Molar ratio of calcium, phosphorus and sodium to potassium in the supernatant for (a) salty whey (UF permeate) and (b) evaporated and filtered salty whey samples at 0 and −24 °C.

Figure 10: Specific heat capacity of NaCl solutions of different concentrations reported in the literature by Chen [26] and that of 26.3 wt% NaCl and salty whey samples measured in this work using the calorimetric probe (OptiMax™ HFCal). Lines are drawn to guide the eye.

Figure 11: Theoretical minimum energy required for processing one tonne of different brine solutions by EFC with 100% water and NaCl recovery. Data for the 5 wt% NaCl ideal case is reported by Verbeek [23].